Paper pulp-based adsorbents for the removal of pharmaceuticals from wastewater: a novel approach towards diversification

Gonçalo Oliveira[a], *Vânia Calisto*[b*], *Sérgio M. Santos*[c], *Marta Otero*[d], *Valdemar I. Esteves*[b]

[a] Department of Chemistry, University of Aveiro, Campus de Santiago, 3810-193 Aveiro, Portugal

[b] Department of Chemistry and CESAM (Centre for Environmental and Marine Studies), University of Aveiro, Campus de Santiago, 3810-193 Aveiro, Portugal

[c] Department of Chemistry and CICECO (Aveiro Institute of Materials), University of Aveiro, Campus de Santiago, 3810-193 Aveiro, Portugal

[d] Department of Environment and Planning and CESAM (Centre for Environmental and Marine Studies), University of Aveiro, Campus de Santiago, 3810-193 Aveiro, Portugal

[*]Corresponding author: E-mail address: vania.calisto@ua.pt

Abstract

In this work, two pulps, bleached (BP) and raw pulp (RP), derived from the paper production process, were used as precursors to produce non-activated and activated carbons (ACs). In the case of non-ACs, the production involved either pyrolysis or pyrolysis followed by acid washing. For ACs production, the pulps were impregnated with K_2CO_3 or H_3PO_4, and then pyrolysed and acid washed. After production, the materials were physically and chemically characterized. Then, batch adsorption tests on the removal of two pharmaceuticals (the anti-epileptic carbamazepine (CBZ) and the antibiotic sulfamethoxazole (SMX)) from ultra-pure water and from Waste Water Treatment Plant (WWTP) effluents were performed. In ultra-pure water, non-ACs were not able to adsorb CBZ or SMX while ACs showed good adsorption capacities. In WWTP effluents, although ACs satisfactorily adsorbed CBZ and SMX, they showed lower adsorption capacities for the latter. Tests with WWTP effluents revealed that the best adsorption capacities were achieved by carbons produced from BP and activated with H_3PO_4: 92 ± 19 mg g^{-1} for CBZ and 13.0 ± 0.6 mg g^{-1} for SMX. These results indicate the potential of paper pulps as precursors for ACs that can be applied in wastewater treatment.

Keywords: Emerging contaminants; Adsorption; Activated carbons; Water treatment; Raw pulp; Bleached pulp.

1. Introduction

The consumption of pharmaceuticals has been increasing considerably over the last decades and with this, their concentration in the environment, mainly aquatic, has grown up too, reaching the μg L^{-1} levels (Jones et al., 2005). The main pathway for the entrance of pharmaceuticals into the environment is the Wastewater Treatment Plants (WWTP) effluents discharge. There is a limited capacity to remove pharmaceuticals from urban wastewaters due to their resistance to conventional treatments. Microorganisms cannot metabolize most drugs as source of carbon (Ren et al., 2018), resulting in the release of contaminated effluents into the aquatic resources that ultimately supply the population (Bahlmann et al., 2014, 2012; Calisto et al., 2011; Rivera-Utrilla et al., 2013)). This fact has been worrying the scientific community, causing the search for new options to solve this serious environmental problem. One of the proposed solutions relies on the implementation of tertiary treatments in WWTP using adsorbent materials, most commonly activated carbons (ACs). In fact, it is well known that adsorption is a very versatile and efficient method to remove contaminants from the environment (Bansal and Goyal, 2005).

ACs are very efficient in adsorption processes, mainly due to very high specific surface areas, most frequently between 800 and 1500 m^2 g^{-1} (Bansal and Goyal, 2005). However, their production is quite expensive since the most common used raw materials are petroleum coke, a product obtained during the oil refining process, and charcoal. Also, these precursors constitute non-renewable resources and originate environmental problems (Wei and Yushin, 2012). The production of adsorbent materials from alternative and renewable raw materials is becoming more and more important in line with the need to adopt processes that promote a more sustainable economy. Adsorbents have been developed from low-cost bio-based raw materials, from diverse origins (Babel, 2003), being agricultural residues the most common type of precursor: cocoa (Saucier et al., 2015) and coconut (Jain et al., 2015) shells, cherry stones (Nowicki et al., 2015), potato peels (Kyzas and Deliyanni, 2015), Isabel grape bagasse (Antunes et al., 2012), coffee residues and almond shells (Flores-Cano et al., 2016), among many others. Adsorbents were also produced from industrial residues like macroalgae waste originated from

agar-agar industry (Ferrera-Lorenzo et al., 2014), carbon residues from woody biomass gasification (Maneerung et al., 2016), cellulose sludge (Orlandi et al., 2017) and sewage sludge of industrial laundries (Silva et al., 2016). One type of substrate that has also been exploited is the sludge resulting from wastewater treatment in the pulp and paper industry (Calisto et al., 2015, 2014; Ferreira et al., 2016; Jaria et al., 2017, 2015; Khalili et al., 2002; Li et al., 2011). Such sludge is produced at a rate of eleven million tons per year in Europe alone (Monte et al., 2009) and its management is an issue of concern for the paper industry. Beyond the abundance of this sludge, it also presents very interesting characteristics as adsorbent precursor, namely high percentage of carbon and volatiles (Azargohar and Dalai, 2008), which are typical of lignocellulosic materials. Raw (RP) and bleached paper pulp (BP) have very similar chemical composition to primary paper mill sludge. Therefore, it could be expected that RP and BP may also have good potential to be used as precursors to generate adsorbents, presenting some advantages in comparison to sludge: (i) their composition is more stable over time; and (ii) they have less inorganic content, which may allow to produce carbons with higher yield and organic carbon content.

The European pulp and paper industry is facing big challenges mainly related to the consumption decay (which is expected to continue due to the digitalization) and to the sector's objectives for the 2050 Roadmap towards a low-carbon bio-economy (Confederation of European Paper Industries, 2014; European Comission, 2013; Presas, 2011). Innovation is essential to cope with these challenges, this involving progressing towards the diversification and exploitation of new businesses, the development of breakthrough technologies, novel products, and applications based on cellulose fibre that generate more added value. In this context, this manuscript aims to evaluate, for the first time, the adequacy of RP and BP from the paper industry as alternative and sustainable precursors of carbonaceous adsorbents. For this purpose, RP and BP were subjected to pyrolysis or pyrolysis combined with chemical activation. The resulting materials were subjected to extensive physico-chemical characterization and applied to the removal of carbamazepine (CBZ) and sulfamethoxazole (SMX) both from ultra-pure water and from the secondary effluent of a local WWTP to assess

the performance of the produced materials in real matrixes. CBZ and SMX were selected because, belonging to two different groups and presenting distinct chemical characteristics, both have large consumption patterns and have been found in natural waters: CBZ is an antiepileptic drug, with a very large global consumption and environmental persistency (Clara et al., 2004), widely detected in aqueous systems (Bahlmann et al., 2014, 2012; Calisto et al., 2011); SMX is the most representative antibiotic of the sulphonamides group, poses bacteriostatic activity, is widely administered in human and veterinary medicine and has been found in water systems (Johnson et al., 2015; Larcher and Yargeau, 2012).

2. Experimental section

2.1. Production of carbon adsorbents

The precursors used in the production of carbon adsorbents were RP and BP, provided by a kraft elemental chlorine free pulp factory, operating using *Eucalyptus globulus* wood. The pulp manufacturing process comprises three main steps: cooking, washing and bleaching (aimed to increase the degree of whiteness by removing or modifying chromophore groups present in the pulp structure). RP and BP were collected before and after the bleaching process, respectively. From the two air dried pulps, twelve different carbons were produced: six from RP and six from BP. Within the six carbons produced from each precursor, two were only pyrolysed (RP500 and RP800 produced from RP; BP500 and BP800 from BP), two other were pyrolysed and then acid washed with HCl 1.2 M (RP500-HCl and RP800-HCl from RP; BP500-HCl and BP800-HCl from BP) and two were activated (either with K_2CO_3 or with H_3PO_4), pyrolysed and acid washed (RP800-HCl-K_2CO_3 and RP800-HCl-H_3PO_4 from RP; BP800-HCl-K_2CO_3 and BP800-HCl-H_3PO_4 from BP). For the activation procedure, the pulp fibres were impregnated with the activating agent in a ratio of 1:1 (*w/w*). For the carbons activated with K_2CO_3, the activating agent was dissolved in distilled water with a proportion of 3:10 (*w/v*) and for H_3PO_4 activation, the activating agent was diluted in a ratio of 1:8 (*v/v*). In both cases, the pulp was impregnated for 1 h with the activating agent solution, using an ultrasonic bath and

then dried at room temperature. The dried pulps (alone or impregnated with the activating agent) were then placed in porcelain crucibles and pyrolysed under nitrogen flow in a furnace muffle that was heated at a rate of 10 ºC min^{-1} up to 500 ºC or 800 ºC, temperatures which were maintained for 150 minutes. Then, also under nitrogen flow, the furnace was allowed to cool until room temperature. After pyrolysis, the ACs and two non-ACs from each pulp were acid washed with HCl 1.2 M (1 L of HCl 1.2 M to 30 mg of carbon adsorbent) and washed with distilled water until washing water reaching neutral pH. After that, all carbons were dried in an oven at 105 ºC for 24 h and crushed mechanically.

2.2. Physical and chemical characterization of raw materials and carbon adsorbents

2.2.1. Total organic carbon (TOC)

TOC was determined for both precursors and for all carbon adsorbents by the difference between total carbon (TC) content and inorganic carbon (IC) content, which were obtained through a TOC analyser (TOC-VCPH Shimadzu, solid sample module SSM-5000A). Carbon content was determined as the average of three replicates.

2.2.2. Thermogravimetric and proximate analysis

The thermogravimetric analysis (TGA) and proximate analyses were made for the precursors and for the produced carbon adsorbents, respectively, and were carried out in a thermogravimetric balance Setsys Evolution 1750, Setaram, TGA mode (S type sensor). Standard methods to determine the moisture (UNE 32002) (AENOR, 1995), volatile matter (UNE 32019) (AENOR, 1985) and ash content (UNE 32004) (AENOR, 1984) were employed. The fixed carbon was determined as the remaining fraction after ash and volatile matter (at dry basis) determination. The experimental procedure for TGA consisted of the sample heating, under nitrogen atmosphere, from room temperature to 105 ºC (heating rate of 10 ºC min^{-1}); sample was kept at this temperature until total stabilization of the weight (approximately 30 min); next, temperature was increased from 105 to 950 ºC (10 ºC min^{-1}), keeping the sample at 950 ºC until total stabilization of the weight (approximately 30 min); finally, at 950 ºC, the

carrier gas was automatically switched to air and the sample was maintained at 950 ºC until total stabilization of the weight. The mass loss observed around 105 ºC is attributed to moisture; the mass loss registered from the end of this first step up to the switching of the carrier gas corresponds to volatile matter; the mass loss comprised between the introduction of the air flow and the stabilization of the weight is attributed to fixed carbon content; and lastly the final residue corresponds to ash content (Valenzuela and Bernalte, 1985).

2.2.3. Elemental analysis

Elemental analysis was determined for the precursors and for all carbon adsorbents. The determination of the samples' content in C, H, N and S was performed in a LECO TruSpec CHNS Micro analyser, using sulfamethazine as calibration standard. The percentage of oxygen was calculated by difference, at a dry and ash free basis.

2.2.4. Fourier transform infrared spectroscopy with attenuated total reflectance (FTIR-ATR)

FTIR-ATR spectra were acquired through a Shimadzu-IRaffinity-1, using an attenuated total reflectance (ATR) module, with a nitrogen purge. The measurements were recorded in the range of 600-4000 cm^{-1} wavenumbers, 4.0 of resolution, 128 scans and with atmosphere and background correction. Both precursors and all produced carbons were analysed.

2.2.5. Point of zero charge (PZC)

The PZC was determined, for the produced carbon adsorbents, by the pH drift method (Aldegs et al., 2008). Briefly, ten solutions of NaCl 0.1 M with pH ranging between 2 and 11 were prepared by adjusting the pH with HCl 0.05 M and 0.1 M and NaOH 0.05 M and 0.1 M. After that, 10 mL of each solution were transferred to a polypropylene tube containing 2 mg of carbon. Each carbon was shaken with the solutions of different initial pH (pH_i), at 40 rpm, overnight at 25 ºC in an overhead shaker (Heidolph, Reax 2). Later, the final pH (pH_f) was measured. The ΔpH ($pH_f - pH_i$) was plotted versus pH_i and PZC was determined as the pH value where the plot crosses the x-axis.

2.2.6. Determination of carbons' functional groups by Boehm's Titration

The quantification of functional groups present on carbons surface was determined by the Boehm's method (Boehm, 1994). Accordingly, each carbon was added to NaOH 0.05 M, $NaHCO_3$ 0.05 M, Na_2CO_3 0.05 M or HCl 0.05 M solutions into polypropylene tubes at a final concentration of 10 g L^{-1}, under nitrogen atmosphere. The mixtures were then shaken inside a thermostatic incubator at 25 °C for 24 h. After, the supernatants were filtered and 25 mL of each one was titrated with 0.1 M HCl or 0.1 M NaOH solutions in order to quantify the total acid and basic functional groups, respectively. In addition, the different acidic groups were determined as follows: the amount of carboxyl groups was estimated by neutralization with $NaHCO_3$ solution; and the amount of phenols was estimated from the difference between the neutralization with NaOH and that determined for the Na_2CO_3 solution. Furthermore, NaOH and HCl solutions were standardized with $C_8H_5KO_4$ and Na_2CO_3, respectively, for the determination of their exact concentration.

2.2.7. Specific surface area (S_{BET})

S_{BET} and total micropore volume (W_0) were determined for carbon adsorbents by nitrogen adsorption isotherms, acquired at 77 K using a Micromeritics Instrument, Gemini VII 2380 after outgassing the materials overnight at 120 ºC. S_{BET} was calculated from the Brunauer-Emmett-Teller equation (Brunauer et al., 1938) in the relative pressure range 0.01-0.1. Total pore volume (V_p) was estimated from the amount of nitrogen adsorbed at a relative pressure of 0.99. W_0 was determined by applying the Dubinin-Radushkevich equation (Marsh and Rand, 1970) to the lower relative pressure zone of the nitrogen adsorption isotherm.

2.2.8. Scanning electron microscopy (SEM)

SEM images were obtained at different magnitudes using a Hitachi SU-70 in order to observe the superficial morphology of the precursors and the produced carbon adsorbents. The magnifications applied were 300x, 1 000x, 3 000x, 10 000x, 30 000x and 50 000x.

206 **2.3. Batch adsorption experiments**

207 In order to test the adsorptive performance of the produced carbons for the removal of
208 pharmaceuticals (namely CBZ and SMX) from water, kinetic and adsorption equilibrium
209 experiments were made under shaking and batch conditions. In all tests, solutions with an initial
210 drug concentration (C_i) of 5 mg L^{-1} were used. Generally, polypropylene tubes containing a
211 known mass of carbon adsorbent together with the drug solution were shaken at 80 rpm in an
212 overhead shaker (Heidolph, Reax 2) at 25 ºC**.** Experiments were run in triplicate. After shaking,
213 each sample was filtered through Whatman PVDF Membrane Filters 0.22 µm to stop the
214 adsorption process. Resulting solutions were analysed by capillary electrophoresis, in order to
215 determine the remaining drug concentration, as described in section 2.3.3. Testing controls,
216 without adsorbents, were also made. Before carrying out kinetic and adsorption equilibrium
217 experiments, preliminary tests were performed with all carbon adsorbents with the purpose of
218 concluding about the materials that have the best adsorptive performances. Based on those
219 studies, only RP800-HCl-H_3PO_4 and BP800-HCl-H_3PO_4 were selected to study their kinetical
220 behaviour and define their isotherms in equilibrium conditions.

221 Ultra-pure water and a final effluent of a WWTP (after secondary treatment, as
222 discharged into the environment) were used for preparing the drug solutions. The effluent was
223 collected from the urban WWTP of *Costa de Lavos* (Figueira da Foz), Portugal; immediately
224 after collection and to remove suspended matter, it was filtered through cellulose Supor-450
225 Membrane Disc Filters 0.45 µm with a vacuum system. After filtration, the samples were stored
226 in the dark at 4 ºC until use, for a maximum period of 10 days. The collected effluent was
227 characterized after filtration. The pH, conductivity and dissolved organic carbon (DOC) content
228 were 7.31, 0.26 ms cm^{-1} and 29.3 ± 0.7 mg L^{-1}, respectively.

229

230 **2.3.1. Kinetic adsorption studies**

231 To study the adsorption kinetics of CBZ and SMX onto the selected carbons, a fixed
232 mass concentration of the carbon adsorbent (g L^{-1}) was employed, varying the contact time

between carbon adsorbents and drug solutions (shaking times of 5, 15, 30, 60, 120 and 240 min). In tests with real effluents, additional shaking times of 8, 10, 14 and 18 h were carried out. For tests with CBZ, the adsorbent mass concentrations used were 0.035 and 0.070 g L^{-1} in ultra-pure water and WWTP effluent, respectively. In the case of SMX, 0.035 and 0.30 g L^{-1} of adsorbent were respectively used for tests in ultra-pure and WWTP effluent. The amount of the target pharmaceutical adsorbed onto the corresponding adsorbent at each shaking time, q_t (mg g^{-1}), was calculated by a mass balance (Equation 1). The experimental data were fitted to the pseudo-first (Lagergren, 1898) and pseudo-second order (Ho et al., 2000) kinetic models (Equations 2 and 3, respectively) in order to determine the kinetic parameters of the experiments.

$$q_t = \frac{(C_i - C_t)}{m} \times V \quad \text{(Equation 1)}$$

$$q_t = q_e\left(1 - e^{-k_1 t}\right) \quad \text{(Equation 2)}$$

$$q_t = \frac{q_e^2 k_2 t}{1 + k_2 q_e t} \quad \text{(Equation 3)}$$

where t is shaking time (min), C_i is the initial concentration of drug (mg L^{-1}), C_t is the remaining drug concentration (mg L^{-1}) after shaking during a time t, m is the mass of adsorbent (g), V is the volume of solution (L), q_e refers to the amount of adsorbate per unit mass of adsorbent at equilibrium (mg g^{-1}), k_1 is the pseudo-first order rate constant (min^{-1}) and k_2 is the pseudo-second order rate constant (g mg^{-1} min^{-1}). GraphPad Prism 5 was used for the nonlinear regression fittings of q_t versus t and three fitting parameters (R^2, ASS and $S_{y/x}$) were determined to evaluate the goodness of fit.

2.3.2. Equilibrium adsorption studies

These experiments were performed using the shaking time needed to attain the equilibrium, as determined in section 2.3.1, varying the concentration of carbon absorbents. The amount of the target pharmaceutical adsorbed onto the corresponding adsorbent q_e (mg g^{-1}), was determined by a mass balance (Equation 4) and the experimental data were fitted to the Langmuir (Langmuir, 1916), Freundlich (Freundlich, 1906) and Langmuir-Freundlich (Sips,

1948) equilibrium models (Equations 5, 6 and 7, respectively) in order to determine the equilibrium parameters of the systems.

$$q_e = \frac{(C_i - C_e)}{m_{ads}} \times V \quad \text{(Equation 4)}$$

$$q_e = \frac{q_m \times K_L \times C_e}{1 + K_L \times C_e} \quad \text{(Equation 5)}$$

$$q_e = K_F \times Ce^{(1/n)} \quad \text{(Equation 6)}$$

$$q_e = \frac{q_{max\,LF} \times K_{LF} Ce^{N_{LF}-1}}{1 + K_{LF} Ce^{N_{LF}-1}} \quad \text{(Equation 7)}$$

where q_m is the maximum adsorbed concentration of adsorbate at the equilibrium (mg g^{-1}), C_e refers to the concentration of adsorbate in the liquid phase at equilibrium (mg L^{-1}), K_L is the Langmuir equilibrium constant (L mg^{-1}), K_F is the Freundlich equilibrium constant (mg g^{-1} (L $mg^{-1})^{1/n}$), n and N_{LF} are the degrees of non-linearity, q_{maxLF} (mg g^{-1}) represents the Langmuir-Freundlich maximum adsorption capacity and K_{LF} (mg g^{-1} (mg $L^{-1})^{-1/N_{LF}}$) is the affinity coefficient of Langmuir-Freundlich model. GraphPad Prism 5 was used for the nonlinear regression fittings of q_e versus C_e and three fitting parameters (R^2, ASS and $S_{y/x}$) were determined to evaluate the goodness of fit.

2.3.3. Drug quantification

The quantification of CBZ and SMX was performed by capillary electrophoresis, using a Beckman P/ACE MDQ (Fullerton, CA, USA) instrument, equipped with a UV/visible detector and controlled by the software 32 Karat. The separation was made using a coated fused silica capillary of 40 cm total length (30 cm to the detection window) using a MEKC (micellar electrokinetic chromatography), as described in Calisto et al., 2015. Three replicates were run for all experiments. Detailed experimental conditions (coating step, analysis parameters and separation method for drug quantification) are presented in Table 1 of Supporting information (SI).

The concentration of CBZ and SMX was determined using a calibration curve in the range between 0.25 and 5.0 mg L^{-1}. Seven standard solutions of each drug were prepared (0.25, 0.50, 1.0, 2.0, 3.0, 4.0 and 5.0 mg L^{-1}) and three replicates of each standard solution were analysed. A linear calibration curve for each new capillary was obtained using the least-squares linear regression.

3. Results and Discussion

3.1. Thermogravimetric analysis of the precursors and production of carbon adsorbents

The thermogravimetric analysis of carbon precursors (RP and BP) was made to determine the mass loss profiles of the pulps and then choose the pyrolysis temperature for each material. The results are presented in Figure S1 of Supporting Information (SI), which shows two stages of mass loss during the pyrolysis of each RP and BP. The first derivative thermogravimetric (DTG) peak of each pulp (76 ºC for RP and 72 ºC for BP) corresponds to the mass loss derived from water evaporation and the second peaks (333 ºC for RP and 356 ºC for BP) are due to the decomposition of organic matter. From these results, it was decided to carry out the pyrolysis of both RP and BP at 500 ºC to ensure the transformation of the organic matter. Moreover, for comparison purposes, pyrolysis of RP and BP was also carried out at 800 ºC because higher temperatures usually translate into a higher development of microporosity, as observed in section 3.2, which is advantageous for adsorbents with superior adsorption capacity (Calisto et al., 2014).

The production yield of all carbon adsorbents was calculated both before and after acid washing. The yields obtained for RP and BP-based carbons varied between 18% and 25% for non-activated and non-washed carbons and between 14% and 21% for non-activated washed carbons, with BP-based carbons registering average yields slightly lower than RP-based carbons. The small decrease verified between non-washed and washed non-activated carbons indicate a low content of inorganic matter (removed by the acidic washing). The largest

311 differences were observed between AC produced from different activating agents, with
312 production yields of 21% and 17% for RP and BP H_3PO_4-ACs, respectively, and 4% and 5% for
313 RP and BP K_2CO_3-ACs, respectively.

314 **3.2. Physical and chemical characterisation of raw materials and carbon adsorbents**

315 TOC results (Table S2 of SI) highlight the low inorganic carbon content present in all
316 produced materials [< 0.6% (*w/w*)], even for non-washed carbons. This constitutes a great
317 advantage for the utilization of these pulps as precursors for carbon adsorbents, considering that
318 AC with high content in inorganic matter often implies lower surface areas and thus lower
319 performance. The TOC of the precursors (between 38 and 40%) highly increased after
320 pyrolysis, reaching contents between 76 and 83% for both non-washed and washed non-
321 activated carbons; and between 59 and 62% for H_3PO_4-AC and 71% for K_2CO_3-AC. Therefore,
322 ACs have less organic carbon (in percentage) than the non-activated carbons; this fact could be
323 explained by the presence of other chemical elements in the surface of the materials (namely
324 oxygen), resulting from the activating agent used, that represent a significant part of material's
325 chemical structure.

326 From proximate and elemental analyses (Table 1), it can be verified a decrease of
327 volatile matter with the increase of pyrolysis temperature, meaning that the carbons produced at
328 higher temperatures released more volatile matter and had more potential for the development
329 of porosity (namely, microporosity). It is also possible to conclude that BP has more potential to
330 develop a porous structure than RP due to its higher content in volatile matter. These facts were
331 proven by the results of S_{BET} and total volume of pores and micropores (Table 2). The presence
332 of a significant percentage of ashes in H_3PO_4-ACs (20.48% for RP800-HCl-H_3PO_4 and 16.55%
333 for BP800-HCl-H_3PO_4) means that activation with H_3PO_4 and pyrolysis of both RP and BP
334 generate a big amount of inorganic material that is not completely removed by the acid washing.
335 A high percentage of ashes in carbon's surface is generally a disadvantage for the carbons
336 because it decreases the adsorptive performance of the materials. However, these values are still
337 lower than those obtained by Jaria et al. (2015) for AC produced by the KOH or NaOH
338 activation of primary sludge, which had about 50% of ashes (*wt.*% dry basis) but showed large

adsorption capacities for the antidepressant fluoxetine. Regarding the elemental analysis, shown in Table 1, it may be concluded that both precursors and carbon adsorbents are mostly constituted by C and O, containing less than 6% of H and negligible amounts of N. The materials have no S in their composition.

The FTIR-ATR spectra of RP, BP and of the produced carbon adsorbents are presented in Figure S2 of SI. The spectra of RP and BP present typical bands of cellulose: bands at ~1030, 1105 and 1160 cm^{-1}, corresponding to cellulosic ethers (C-O-C bonds); band at ~1053 is attributed to C-OH stretch of primary alcohols and carbohydrates (Boehm, 1994; Marsh and Rand, 1970). All these bands disappeared in the materials pyrolysed at 500 ºC. This is consistent with the thermogravimetric results of the precursors (Figure S1 of SI), where the decomposition of the most thermo-labile fraction of organic matter, as cellulose, occurs between 300 and 400 ºC. There are also two bands in BP and RP spectra that are eliminated with pyrolysis: ~2890 and 3330 cm^{-1} which represent C-H stretch vibrations and –OH phenol, respectively (Ahmad et al., 2007). In carbon adsorbent materials, several bands between 1660 and 2000 cm^{-1} appeared, which are related with the presence of some aromatic combination bands (Coates, 2006). The bands at ~1508 and 1339 cm^{-1} correspond to aromatic ring stretches (Marsh and Rand, 1970; Yang et al., 2007). All bands in this region are typical of the presence of aromatic groups, which constitute the main structure of AC. The presence of some bands at 3400-4000 cm^{-1} region in all produced carbons is also notable and related with OH stretching (Yang et al., 2007).

The PZC was determined in order to know the net charge of each carbon (see Figure S3 of SI). Also, the concentration of some functional groups, namely carboxyl, phenols and total basic groups were obtained through Boehm's Titration. Figure 1 relates the PZC with the obtained functional groups concentrations for all produced carbon adsorbents. Since carboxyls and phenols are acidic groups, the low PZCs is directly connected with the presence of high concentrations of these two functional groups. On the other hand, higher PZCs are linked to a higher concentration of total basic groups and lower concentration of both carboxyl and phenol groups.

366 The S_{BET} results (Table 2) revealed large differences between non-activated and ACs,
367 highlighting the importance of the activation step in the development of higher porosity and
368 S_{BET}. Except for those activated with K_2CO_3, all the carbons produced in the same conditions
369 presented higher S_{BET} for BP-based carbons, compared with RP-based carbons. This fact may be
370 explained by the higher content of volatile matter in BP in comparison with RP, as mentioned
371 before. It is noteworthy that, despite similar S_{BET}, H_3PO_4-ACs have a microporous volume (W_0)
372 much higher than K_2CO_3-ACs, which will certainly influence the adsorptive capacity of these
373 materials. For comparison purposes, the results determined for a commercially available AC
374 (PBFG4, kindly provided by Chemviron Carbon) were also included in Table 2. A complete
375 physical and chemical characterization of PBFG4 can be found in previous works (Calisto et al.,
376 2014; Jaria et al., 2015). As it may be seen, S_{BET} values for the ACs produced in this study are
377 very close or even higher (in the case of BP800-H_3PO_4-HCl) than that of PBFG4. However, W_0
378 is significantly higher for the commercial AC (PBFG4) than for the here produced adsorbents.
379 The SEM analysis of the raw materials and produced carbon adsorbents are presented in
380 Tables S3-S6 of SI at different magnifications. Figures 2 and 3 present images of both
381 precursors and some examples of RP and BP-based carbons. The images show a gradual
382 difference between the surface morphology of the precursors, where the cellulose fibres are
383 intact, and the non-activated and non-washed carbons, where the fibres exhibit some degree of
384 destruction with no evident porosity (as confirmed by S_{BET} analysis) and finally the AC, where a
385 much more modified surface and a well-developed porosity are observable. This fact is
386 consistent with the results of S_{BET}, V_p and W_0. Regarding ACs, it is possible to verify a huge
387 difference in the morphology between carbons activated with K_2CO_3 and with H_3PO_4. K_2CO_3-
388 ACs have a rough surface with a very noticeable porosity while H_3PO_4-ACs have a smoother
389 surface, giving the impression that the fibres of the raw materials were barely affected. Still,
390 both activating agents resulted in carbon adsorbents with similar S_{BET}, with H_3PO_4-ACs having
391 a much higher microporous volume. A possible explanation for the non-observed porosity in
392 H_3PO_4-ACs SEM images could be the existence of a high number of micropores in these
393 carbons, when compared with K_2CO_3-ACs, which are not visible at the used magnification.

3.3. Batch adsorption experiments

Preliminary tests, performed in ultra-pure water, revealed no adsorption of the studied pharmaceuticals onto the non-ACs, even at mass concentrations up to 10 times higher than those used for the same tests with ACs. This performance is, in fact, in accordance to S_{BET} results. Therefore, kinetic and equilibrium studies were not performed with non-ACs.

Concerning the performance of the produced ACs in the preliminary experiments, H_3PO_4-ACs systematically presented better percentages for CBZ and SMX removal than K_2CO_3-ACs. Better removal percentages of H_3PO_4-ACs should be related with the total pore and micropore volumes, which are much higher than those obtained for K_2CO_3-ACs (Table 2). Moreover, the lower PZCs and a more acidic carbon surface may also be determinant factors for a better performance, since H_3PO_4-ACs have higher concentrations of carboxyl and phenol groups in their structure, in comparison with K_2CO_3-ACs (Figure 1). Based on these results, it was decided to use the two H_3PO_4-ACs (RP800-HCl-H_3PO_4 and BP800-HCl-H_3PO_4) to perform the kinetic and equilibrium studies.

3.3.1. Kinetic adsorption studies

Kinetic studies for the adsorption of CBZ and SMX onto RP800-HCl-H_3PO_4 and BP800-HCl-H_3PO_4 were performed in ultra-pure water and in WWTP effluents. The amount of CBZ and SMX adsorbed (q_t, mg g^{-1}) is represented *versus* shaking time (t) in Figure 4.

The parameters determined by the fittings of kinetic models (Equations 2 and 3) to experimental results are summarized in Table 3. For the fitting parameters, R^2, $S_{y/x}$ and ASS, pseudo-second order was the model that best fitted the experimental results on the adsorption of both CBZ and SMX. Then, it was possible to conclude that the adsorption of both CBZ and SMX was much faster (higher k_2) in ultra-pure water than in the WWTP effluent. It was also proven that the difference between the adsorption kinetics in ultra-pure water and WWTP effluents was more noticeable in tests with CBZ than with SMX. In fact, CBZ adsorption onto

RP800-H_3PO_4-HCl and BP800-H_3PO_4-HCl was ten and thirteen times faster, respectively, in ultra-pure water than in WWTP effluents. These results are probably related to the complex chemical composition of the secondary WWTP effluent, which contains organic and inorganic components (such as dissolved organic matter) that can compete for the adsorption sites of the carbons and, in this way, decrease the adsorption kinetics and hamper the access to the pores of the adsorbents. In tests with SMX, BP800-H_3PO_4-HCl adsorbed just twice faster in ultra-pure water, while RP800-H_3PO_4-HCl displayed faster adsorption kinetics in WWTP effluents. Regarding the produced ACs, adsorption of both CBZ and SMX was faster (please, see higher k_2 in Table 3) onto BP800-H_3PO_4-HCl than onto RP800-H_3PO_4-HCl either from ultra-pure water or from the WWTP effluent.

The comparison of adsorption kinetics of the here produced adsorbents with a literature study, that used, under the same experimental conditions, a commercial AC (PBFG4) for the removal of CBZ and SMX from ultra-pure water (see Table 3) (Calisto et al., 2015), revealed that the adsorption kinetics were faster for BP800-H_3PO_4-HCl (higher k_2), proving the good potential of this type of precursors to produce ACs with good adsorptive properties.

3.3.2. Equilibrium adsorption studies

Equilibrium adsorption tests were performed for CBZ and SMX, both in ultra-pure water and WWTP effluents. The amount of CBZ and SMX adsorbed (q_e, mg g^{-1}), both in ultra-pure water and WWTP effluents, is represented *versus* the remaining concentration of drug in solution (C_e) in Figure 5. The parameters obtained from the fittings of experimental results to the considered equilibrium models (Equations 5, 6 and 7) are summarized in Table 3.

The best fit was obtained for the Langmuir-Freundlich equilibrium model, according to the three selected fitting parameters (R^2, $S_{y/x}$ and ASS) displayed in Table 3. From the analysis of the fitted parameters for the Langmuir-Freundlich equilibrium model, it is possible to conclude that, except for SMX adsorption onto RP800-HCl-H_3PO_4 from ultra-pure water, the maximum adsorptive capacities (q_m) were always higher for BP-based ACs than for RP-based

448 ACs. These results are partially justified by the higher S_{BET} of BP800-HCl-H_3PO_4 (965 m^2 g^{-1}),
449 comparing with RP800-HCl-H_3PO_4 (768 m^2 g^{-1}). On the other hand, equilibrium experiments in
450 ultra-pure water present better or similar q_m for SMX than for CBZ. Contrarily, in WWTP
451 effluents, q_m was significantly higher for CBZ than for SMX. In any case, for these drugs, the
452 adsorptive capacity of both BP800-HCl-H_3PO_4 and RP800-HCl-H_3PO_4 was higher in ultra-pure
453 water than in real effluents due to the presence of organic matter or other competitors in the
454 latter. Yet, the decrease of carbons adsorptive capacity in WWTP effluent was much more
455 noticeable for SMX than for CBZ. In the case of CBZ, the adsorptive capacities of the
456 adsorbents just decreased 45% and 14%, using RP800-HCl-H_3PO_4 and BP800-HCl-H_3PO_4,
457 respectively, while for SMX, the adsorptive capacities decreased 92% and 87% for the same
458 carbon adsorbents, respectively. It was hypothesised that the reason for this accentuated
459 decrease may lie in the carbon surface chemistry. Since the PZC of H_3PO_4-ACs is quite low (2.3
460 for BP800-HCl-H_3PO_4 and 2.8 for RP800-HCl-H_3PO_4) and the pH of collected WWTP effluent
461 was 7.31, the functional groups present in the carbon surface are deprotonated, resulting in a
462 negatively charged carbon, attracting cations and repulsing anions. Due to the pH of the WWTP
463 effluent, SMX was negatively charged in these tests (pKa_1=1.8; pKa_2=5.7 (Calisto et al., 2015)),
464 which induced a repulsion between the drug and the groups present on the carbon surface,
465 making difficult the adsorption process. The dissociation equilibrium and speciation diagram of
466 SMX are schematized in Figure 6.
467 In ultra-pure water, which has a more acidic pH than WWTP effluents (between 5.5 and
468 6.0), there is an equilibrium between the neutral and negative species of SMX because pKa_2 of
469 SMX is 5.7. With the presence of the neutral form of SMX, no electrostatic repulsion forces
470 between the neutral drug and the adsorbent surface occur, which further potentiates the
471 adsorption in this matrix. Then, the absence of competitors in ultra-pure water also favours the
472 SMX adsorption onto the produced carbon adsorbents.
473 The pH-dependent effect was not felt in CBZ adsorption experiments because CBZ has
474 a neutral charge at both the pH of ultra-pure water and WWTP effluents (pKa=13.9 (Calisto et
475 al., 2015)). Therefore, in this case, the observed differences between the adsorption capacities

obtained between ultra-pure water and WWTP effluents are mainly due to the competition effect of substances present in the effluents.

For comparison purposes, the results obtained under the same experimental conditions for the removal of CBZ and SMX from ultra-pure water with a commercial AC (PBFG4) (Calisto et al., 2015), are summarized in Table 3. The results show that the adsorption capacities obtained with PBFG4 and the carbon adsorbents produced in this work are quite similar, particularly in the case of BP800-H_3PO_4-HCl. Therefore, despite the total microporous volume of PBFG4 being three times higher than that of BP800-H_3PO_4-HCl (please see Table 2), maximum adsorption capacities of PBFG4 were only 1.2 and 1.1 times higher than those of BP800-H_3PO_4-HCl for CBZ and SMX, respectively.

On the basis of the kinetic and equilibrium results, it is possible to conclude that BP800-H_3PO_4-HCl was, among the here produced materials, the carbon adsorbent with the best adsorptive performance, being comparable to that of a commercial AC used under identical experimental conditions.

4. Conclusions

This study evaluated the adequacy of RP and BP as alternative and renewable-origin precursors to produce high efficiency carbon adsorbents to remove pharmaceuticals from water. The results obtained revealed that non-ACs produced from RP and BP have no potential for this application, with negligible microporous structure and no ability to remove the tested pharmaceuticals from ultra-pure water. On the other hand, the activation of RP and BP with K_2CO_3 and H_3PO_4 allowed to produce carbon adsorbents with high adsorptive performances for CBZ and SMX, with interesting physical and chemical characteristics such as a high S_{BET} and a high total volume of pores and micropores, mainly for BP800-HCl-H_3PO_4 (S_{BET} of 965 m^2 g^{-1}, V_p and W_0 of 0.41 and 0.11 cm^2, respectively). By studying the kinetic and equilibrium behaviour of H_3PO_4-ACs for the adsorption of CBZ and SMX in ultra-pure water and WWTP effluents, it was possible to conclude that the adsorption was slower and the capacity lower in the WWTP effluents than in ultra-pure water. Differences should be related to the presence of

competitors that influence the adsorption process in WWTP effluents and to pH effects, particularly in the case of SMX. In general, among the produced adsorbents, the one from BP and activated with H_3PO_4 (BP800-HCl-H_3PO_4) displayed the best adsorptive performance, which was comparable to that of a commercial AC. Therefore, it was here proved the potential of pulp as precursor to produce adsorbents with high performance, which opens a new research line towards diversification in the paper industry.

Acknowledgements

This work was funded by FEDER through COMPETE 2020 and by national funds through FCT by the research project PTDC/AAG-TEC/1762/2014. Thanks are due for the financial support to CESAM (UID/AMB/50017-POCI-01-0145-FEDER-007638), to FCT/MCTES through national funds (PIDDAC), and the co-funding by the FEDER, within the PT2020 Partnership Agreement and Compete 2020. The work was also developed within the scope of the project CICECO - Aveiro Institute of Materials, POCI-01-0145-FEDER-007679 (UID/CTM/50011/2013), financed by national funds through the FCT/MEC. Vânia Calisto thanks FCT for her postdoctoral grant (SFRH/BPD/78645/2011). Marta Otero and Sérgio Santos thank support by the FCT Investigator Program (IF/00314/2015 and IF/00973/2014, respectively). The authors acknowledge the kind collaboration of Cláudia Guerreiro and Maria Miguel from the company "Luságua" for support with effluent collection.

References

AENOR: Norma UNE 32002:1995. http://www.aenor.es/.

AENOR: Norma UNE 32019:1985. http://www.aenor.es/.

AENOR: Norma UNE 32004:1984. http://www.aenor.es/.

Ahmad, A., Loh, M., Aziz, J., 2007. Preparation and characterization of activated carbon from oil palm wood and its evaluation on Methylene blue adsorption. Dyes Pigments 75, 263–272.

Aldegs, Y., Elbarghouthi, M., Elsheikh, A., Walker, G., 2008. Effect of solution pH, ionic

strength, and temperature on adsorption behavior of reactive dyes on activated carbon. Dyes Pigments 77, 16–23.

Antunes, M., Esteves, V.I., Guégan, R., Crespo, J.S., Fernandes, A.N., Giovanela, M., 2012. Removal of diclofenac sodium from aqueous solution by Isabel grape bagasse. Chem. Eng. J. 192, 114–121.

Azargohar, R., Dalai, A.K., 2008. Steam and KOH activation of biochar: Experimental and modeling studies. Micropor. Mesopor. Mat. 110, 413–421.

Babel, S., 2003. Low-cost adsorbents for heavy metals uptake from contaminated water: a review. J. Hazard. Mater. 97, 219–243.

Bahlmann, A., Brack, W., Schneider, R.J., Krauss, M., 2014. Carbamazepine and its metabolites in wastewater: Analytical pitfalls and occurrence in Germany and Portugal. Water Res. 57, 104–114.

Bahlmann, A., Carvalho, J.J., Weller, M.G., Panne, U., Schneider, R.J., 2012. Immunoassays as high-throughput tools: Monitoring spatial and temporal variations of carbamazepine, caffeine and cetirizine in surface and wastewaters. Chemosphere 89, 1278–1286.

Bansal, R.C., Goyal, M., 2005. Activated carbon adsorption. Taylor & Francis Group.

Boehm, H.P., 1994. Some aspects of the surface chemistry of carbon blacks and other carbons. Carbon 32, 759–769.

Brunauer, S., Emmett, P.H., Teller, E., 1938. Adsorption of gases in multimolecular layers. J. Am. Chem. Soc. 60, 309–319.

Calisto, V., Bahlmann, A., Schneider, R.J., Esteves, V.I., 2011. Application of an ELISA to the quantification of carbamazepine in ground, surface and wastewaters and validation with LC–MS/MS. Chemosphere 84, 1708–1715.

Calisto, V., Ferreira, C.I.A., Oliveira, J.A.B.P., Otero, M., Esteves, V.I., 2015. Adsorptive removal of pharmaceuticals from water by commercial and waste-based carbons. J. Environ. Manage. 152, 83–90.

Calisto, V., Ferreira, C.I.A., Santos, S.M., Gil, M.V., Otero, M., Esteves, V.I., 2014. Production of adsorbents by pyrolysis of paper mill sludge and application on the removal of

559 citalopram from water. Bioresource Technol. 166, 335–344.
560 Clara, M., Strenn, B., Kreuzinger, N., 2004. Carbamazepine as a possible anthropogenic marker
561 in the aquatic environment: investigations on the behaviour of Carbamazepine in
562 wastewater treatment and during groundwater infiltration. Water Res. 38, 947–954.
563 Coates, J., 2006. Interpretation of Infrared Spectra, A Practical Approach, in: Encyclopedia of
564 Analytical Chemistry. John Wiley & Sons, Ltd, Chichester, UK.
565 Confederation of European Paper Industries, 2014. Resource efficiency in the pulp and paper
566 industry: making more from our natural resources.
567 Dias, I.N., Souza, B.S., Pereira, J.H.O.S., Moreira, F.C., Dezotti, M., Boaventura, R.A.R., Vilar,
568 V.J.P., 2014. Enhancement of the photo-Fenton reaction at near neutral pH through the use
569 of ferrioxalate complexes: A case study on trimethoprim and sulfamethoxazole antibiotics
570 removal from aqueous solutions. Chem. Eng. J. 247, 302–313.
571 European Comission, 2013. Pulp and paper industry [WWW Document]. URL:
572 https://ec.europa.eu/growth/sectors/raw-materials/industries/forest-based/pulp-paper_en
573 (accessed 12.12.17).
574 Ferreira, C.I.A., Calisto, V., Otero, M., Nadais, H., Esteves, V.I., 2016. Comparative adsorption
575 evaluation of biochars from paper mill sludge with commercial activated carbon for the
576 removal of fish anaesthetics from water in Recirculating Aquaculture Systems. Aquac.
577 Eng. 74, 76–83.
578 Ferrera-Lorenzo, N., Fuente, E., Suárez-Ruiz, I., Ruiz, B., 2014. KOH activated carbon from
579 conventional and microwave heating system of a macroalgae waste from the Agar–Agar
580 industry. Fuel Process. Technol. 121, 25–31.
581 Flores-Cano, J.V., Sánchez-Polo, M., Messoud, J., Velo-Gala, I., Ocampo-Pérez, R., Rivera-
582 Utrilla, J., 2016. Overall adsorption rate of metronidazole, dimetridazole and diatrizoate on
583 activated carbons prepared from coffee residues and almond shells. J. Environ. Manage.
584 169, 116–125.
585 Freundlich, H., 1906. Over the adsorption in solution. J. Phy. Chem. 57, 385-470.
586 H. Jones, O.A., Voulvoulis, N., Lester, J.N., 2005. Human harmaceuticals in wastewater

587 treatment processes. Crit. Rev. Environ. Sci. Technol. 35, 401–427.
588 Ho, Y.S., McKay, G., Wase, D.A.J., Forster, C.F., 2000. Study of the sorption of divalent metal
589 ions on to peat. Adsorpt. Sci. Technol. 18, 639–650.
590 Jain, A., Balasubramanian, R., Srinivasan, M.P., 2015. Production of high surface area
591 mesoporous activated carbons from waste biomass using hydrogen peroxide-mediated
592 hydrothermal treatment for adsorption applications. Chem. Eng. J. 273, 622–629.
593 Jaria, G., Calisto, V., Gil, M.V., Otero, M., Esteves, V.I., 2015. Removal of fluoxetine from
594 water by adsorbent materials produced from paper mill sludge. J. Colloid Interface Sci.
595 448, 32–40.
596 Jaria, G., Silva, C.P., Ferreira, C.I.A., Otero, M., Calisto, V., 2017. Sludge from paper mill
597 effluent treatment as raw material to produce carbon adsorbents: An alternative waste
598 management strategy. J. Environ. Manage. 188, 203–211.
599 Johnson, A.C., Keller, V., Dumont, E., Sumpter, J.P., 2015. Assessing the concentrations and
600 risks of toxicity from the antibiotics ciprofloxacin, sulfamethoxazole, trimethoprim and
601 erythromycin in European rivers. Sci. Total Environ. 511, 747–755.
602 Khalili, N., Vyas, J., Weangkaew, W., Westfall, S., Parulekar, S., Sherwood, R., 2002.
603 Synthesis and characterization of activated carbon and bioactive adsorbent produced from
604 paper mill sludge. Sep. Purif. Technol. 26, 295–304.
605 Kyzas, G.Z., Deliyanni, E.A., 2015. Modified activated carbons from potato peels as green
606 environmental-friendly adsorbents for the treatment of pharmaceutical effluents. Chem.
607 Eng. Res. Des. 97, 135–144.
608 Lagergren, S., 1898. About the theory of so-called adsorption of soluble substances. *Kungliga*
609 *Svenska Vetenskapsakademiens*, 24, 1-39.
610 Langmuir, I., 1916. The constitution and fundamental properties of solids and liquids. J. Am.
611 Chem. Soc. 38, 2221–2295.
612 Larcher, S., Yargeau, V., 2012. Biodegradation of sulfamethoxazole: current knowledge and
613 perspectives. Appl. Microbiol. Biotechnol. 96, 309–318.
614 Li, W.-H., Yue, Q.-Y., Gao, B.-Y., Wang, X.-J., Qi, Y.-F., Zhao, Y.-Q., Li, Y.-J., 2011.

615 Preparation of sludge-based activated carbon made from paper mill sewage sludge by
616 steam activation for dye wastewater treatment. Desalination 278, 179–185.
617 Maneerung, T., Liew, J., Dai, Y., Kawi, S., Chong, C., Wang, C.-H., 2016. Activated carbon
618 derived from carbon residue from biomass gasification and its application for dye
619 adsorption: Kinetics, isotherms and thermodynamic studies. Bioresource Technol. 200,
620 350–359.
621 Marsh, H., Rand, B., 1970. The characterization of microporous carbons by means of the
622 dubinin-radushkevich equation. J. Colloid Interface Sci. 33, 101–116.
623 Monte, M.C., Fuente, E., Blanco, A., Negro, C., 2009. Waste management from pulp and paper
624 production in the European Union. Waste Manag. 29, 293–308.
625 Nowicki, P., Kazmierczak, J., Pietrzak, R., 2015. Comparison of physicochemical and sorption
626 properties of activated carbons prepared by physical and chemical activation of cherry
627 stones. Powder Technol. 269, 312–319.
628 Orlandi, G., Cavasotto, J., Machado, F.R.S., Colpani, G.L., Magro, J.D., Dalcanton, F., Mello,
629 J.M.M., Fiori, M.A., 2017. An adsorbent with a high adsorption capacity obtained from
630 the cellulose sludge of industrial residues. Chemosphere 169, 171–180.
631 Presas, T., 2011. The pulp and paper industry: intelligent use of raw materials, in: European
632 Economic and Social Committee. Brussels.
633 Ren, X., Zeng, G., Tang, L., Wang, J., Wan, J., Liu, Y., Yu, J., Yi, H., Ye, S., Deng, R., 2018.
634 Sorption, transport and biodegradation – An insight into bioavailability of persistent
635 organic pollutants in soil. Sci. Total Environ. 610-611, 1154-1163.
636 Rivera-Utrilla, J., Sánchez-Polo, M., Ferro-García, M.Á., Prados-Joya, G., Ocampo-Pérez, R.,
637 2013. Pharmaceuticals as emerging contaminants and their removal from water: a review.
638 Chemosphere 93, 1268–1287.
639 Saucier, C., Adebayo, M.A., Lima, E.C., Cataluña, R., Thue, P.S., Prola, L.D.T., Puchana-
640 Rosero, M.J., Machado, F.M., Pavan, F.A., Dotto, G.L., 2015. Microwave-assisted
641 activated carbon from cocoa shell as adsorbent for removal of sodium diclofenac and
642 nimesulide from aqueous effluents. J. Hazard. Mater. 289, 18–27.

643 Silva, T.L., Ronix, A., Pezoti, O., Souza, L.S., Leandro, P.K.T., Bedin, K.C., Beltrame, K.K.,
644 Cazetta, A.L., Almeida, V.C., 2016. Mesoporous activated carbon from industrial laundry
645 sewage sludge: Adsorption studies of reactive dye Remazol Brilliant Blue R. Chem. Eng.
646 J. 303, 467–476.
647 Sips, R., 1948. On the Structure of a Catalyst Surface. J. Chem. Phys. 16, 490–495.
648 Teixeira, S., Delerue-Matos, C., Santos, L., 2012. Removal of sulfamethoxazole from solution
649 by raw and chemically treated walnut shells. Environ. Sci. Pollut. Res. 19, 3096–3106.
650 Valenzuela, C., Bernalte, A., 1985. Un método termogravimétrico rápido para análisis
651 inmediato de carbones. Boletín Geológico y Min. 58–61.
652 Wei, L., Yushin, G., 2012. Nanostructured activated carbons from natural precursors for
653 electrical double layer capacitors. Nano Energy 1, 552–565.
654 Yang, H., Yan, R., Chen, H., Lee, D.H., Zheng, C., 2007. Characteristics of hemicellulose,
655 cellulose and lignin pyrolysis. Fuel 86, 1781–1788.

Table

Click here to download Table: tables.docx

Tables

Table 1 – Proximate and elemental analyses for precursors and carbon materials

Sample	Proximate analysis (*wt.*%, dry basis)					Elemental analysis (*wt.*%, dry and ash free basis)				
	Moisture	Volatile Matter (VM)	Fixed Carbon (FC)	Ash	VM/ FC	% C	% H	% N	% S	% O *
RP	6.13	79.77	19.29	0.94	4.14	41.60	5.93	-	-	52.47
BP	6.88	87.75	11.72	0.53	7.49	42.34	5.99	0.03	-	51.63
RP500	4.83	21.54	74.92	3.54	0.29	79.42	2.44	-	-	18.15
BP500	3.11	27.91	72.09	-	0.39	81.30	2.28	-	-	16.41
RP800	8.37	11.38	82.96	5.66	0.14	82.70	0.96	0.05	-	16.29
BP800	6.02	8.89	90.57	0.53	0.10	83.93	0.23	-	-	15.85
RP500-HCl	4.94	19.61	79.84	0.55	0.25	77.56	2.77	-	-	19.67
BP500-HCl	4.61	19.51	79.56	0.93	0.25	78.91	2.20	-	-	18.89
RP800-HCl	8.38	7.71	91.11	1.17	0.08	85.69	-	0.12	-	14.19
BP800-HCl	8.04	7.50	91.78	0.72	0.08	84.88	-	-	-	15.12
RP800-HCl-K_2CO_3	14.92	11.72	87.84	0.44	0.13	72.79	-	-	-	27.21
BP800-HCl-K_2CO_3	16.36	14.64	85.36	0.00	0.17	71.82	0.94	0.05	-	27.18
RP800-HCl-H_3PO_4	17.67	23.96	55.56	20.48	0.43	68.93	1.69	-	-	29.38
BP800-HCl-H_3PO_4	14.37	27.12	56.33	16.55	0.48	73.58	4.04	-	-	22.37

*** - calculated by difference**

Table 2 – Specific surface area (S_{BET}), total pore volume (V_p), total micropore volume (W_0) and average pore diameter (D) of all produced materials. For comparison purposes, data are also presented for PBFG4, a commercially available AC (from Calisto et al., 2014).

Carbon adsorbent	S_{BET} (m^2g^{-1})	V_p (cm^3g^{-1})	W_0 (cm^3g^{-1})	D (nm)
RP500	3	0.002	0.000	19.00
BP500	6	0.010	0.000	7.26
RP800	3	0.003	0.001	7.90
BP800	5	0.001	0.000	9.43
RP500-HCl	6	0.004	0.001	5.95
BP500-HCl	27	0.009	0.001	5.18
RP800-HCl	27	0.003	0.001	5.17
BP800-HCl	56	0.010	0.001	5.20
RP800-HCl -K_2CO_3	855	0.065	0.018	2.69
BP800-HCl -K_2CO_3	814	0.056	0.015	2.66
RP800-HCl -H_3PO_4	768	0.311	0.137	2.33
BP800-HCl -H_3PO_4	965	0.408	0.108	2.59
PBFG4 (Calisto et al., 2014)	848	0.360	0.295	0.84

Table 3 - Fitting parameters of pseudo-first and pseudo-second order kinetic models and of Langmuir, Freundlich and Langmuir-Freundlich equilibrium models for experimental results on the adsorption of CBZ and SMX, onto RP800-HCl-H_3PO_4 and BP800-HCl-H_3PO_4 in ultra-pure water and WWTP effluents.

		CBZ					**SMX**				
		Ultra-pure water			**WWTP effluent**		**Ultra-pure water**			**WWTP effluent**	
		RP800-H_3PO_4-HCl	BP800-H_3PO_4-HCl	PBFG4 (Calisto et al., 2015)	RP800-H_3PO_4-HCl	BP800-H_3PO_4-HCl	RP800-H_3PO_4-HCl	BP800-H_3PO_4-HCl	PBFG4 (Calisto et al., 2015)	RP800-H_3PO_4-HCl	BP800-H_3PO_4-HCl
Kinetic studies											
Pseudo 1st order	q_e (mg g^{-1})	56±4	85±3	122±3	25±3	51±3	83±3	95±3	110±3	5.3±0.6	13.0±0.9
	k_1 (min^{-1})	0.01±0.03	0.26±0.06	0.10±0.01	0.006±0.002	0.015±0.004	0.058±0.007	0.19±0.037	0.15±0.02	0.017±0.007	0.021±0.006
	R^2	0.901	0.968	0.989	0.813	0.874	0.984	0.972	0.978	0.789	0.870
	$S_{y/x}$	7.375	6.234	5.349	4.165	6.945	4.602	6.622	6.674	1.025	1.829
	ASS	271.9	194.3	-	156.1	385.8	84.71	219.3	-	7.357	26.77
Pseudo 2nd order	q_e (mg g^{-1})	61±3	90±2	132±3	29±3	56±3	90±2	101±2	117±3	6.0±0.6	14.0±0.8
	k_2 (g mg^{-1} min^{-1})	0.0030±0.0009	0.005±0.001	0.0011±0.0002	0.0003±0.0001	0.0004±0.0001	0.00089±0.00009	0.0030±0.003	0.0021±0.0004	0.004±0.002	0.0020±0.007
	R^2	0.960	0.990	0.993	0.862	0.935	0.996	0.996	0.991	0.876	0.936
	$S_{y/x}$	4.712	3.494	4.253	3.852	4.979	2.173	2.528	4.387	0.785	1.279
	ASS	111.0	61.04	-	115.4	198.3	18.89	31.95	-	4.314	13.10
Equilibrium studies											
Langmuir	q_m (mg g^{-1})	57±2	93±2	116±3	29.9±0.5	80±3	93±1	110±4	118±5	8.8±0.2	13.3±0.5
	K_L (L mg^{-1})	9±4	3.2±0.4	10±2	5.5±0.6	2.2±0.4	4.5±0.4	5.0±0.7	2.3±0.4	55±37	13±3
	R^2	0.972	0.991	0.9906	0.991	0.978	0.997	0.985	0.9819	0.987	0.961
	$S_{y/x}$	3.111	2.742	3.972	0.876	3.420	1.659	4.215	4.744	0.374	0.907
	ASS	67.74	52.64	-	6.905	105.3	19.27	124.3	-	0.838	5.759
Freundlich	K_F ($mg^{1-1/n}$ $L^{1/N}$ g^{-1})	48±2	67±1	102.7±0.8	23.6±0.6	52±2	72.6±0.7	88±3	78±2	8.6±0.2	11.5±0.5
	n	12±5	4.0±0.4	9.1±0.7	6.0±0.9	3.6±0.4	5.3±0.3	5±1	3.1±0.2	67±92	10±4
	R^2	0.965	0.988	0.998	0.969	0.971	0.996	0.956	0.987	0.983	0.918
	$S_{y/x}$	3.479	3.144	2.011	1.620	3.918	1.828	7.213	4.031	0.426	1.317
	ASS	84.72	69.19	-	23.63	138.2	23.40	364.2	-	1.091	12.13
Langmuir - Freundlich	q_m (mg g^{-1})	54±4	107±21	Ambiguous fitting	30±1	92±19	106±14	102±4	Ambiguous fitting	8.7±0.2	13.0±0.6
	K_{LF} (mg g^{-1} (mg L^{-1})$^{-1/N_{LF}}$)	12±19	2±1		5±2	1.4±0.7	2±1	11±6		$1.38x10^{-6}$±$9x10^{-8}$	22±25
	n_{LF}	0.8±0.8	1.4±0.5		1.1±0.2	1.4±0.4	1.6±0.5	0.7±0.2		0±7	0.8±0.4
	R^2	0.972	0.993		0.991	0.981	0.998	0.990		0.990	0.963

	$S_{y/x}$	3.336	2.724		0.923	3.370	1.461	3.698	0.357	0.950
	ASS	66.75	44.53		6.820	90.88	12.81	82.05	0.637	5.417

Figure Captions

Figure 1 – Point of zero charge (PZC) and functional groups concentrations of the produced carbon adsorbents

Figure 2 - SEM images of RP, RP-800 and RP800-HCl-K_2CO_3 (from left to right) at 10 000x

Figure 3 - SEM images of BP at 3 000x, BP-800 and BP800-HCl- H3PO4 at 10 000x (from left to right)

Figure 4 – Experimental kinetic results and nonlinear fittings of the pseudo-second order kinetic model (best fit) corresponding to the adsorption of CBZ and SMX onto RP800-HCl-H_3PO_4 and BP800-HCl-H_3PO_4, from ultra-pure water or WWTP effluents

Figure 5 – Experimental equilibrium results and nonlinear fittings of the Langmuir-Freundlich model (best fit) corresponding to the adsorption of CBZ and SMX onto RP800-HCl-H_3PO_4 and BP800-HCl-H_3PO_4, from either ultra-pure water or WWTP effluents

Figure 6 – Dissociation equilibrium and speciation diagram of SMX (adapted from Teixeira et al., 2012 and Dias et al., 2014)

Figure 1 b&w

Click here to download high resolution image

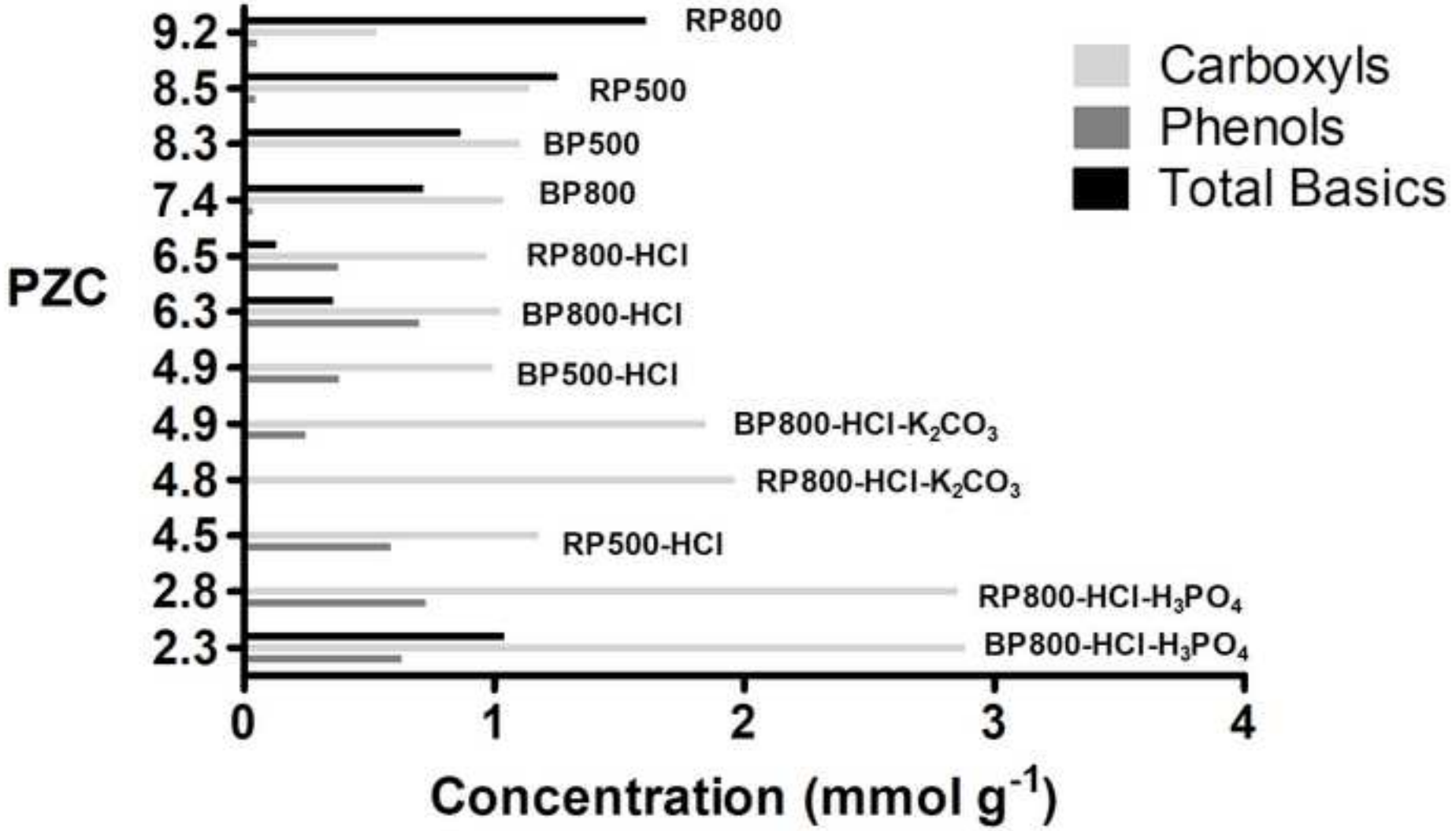

Figure 1 color

Click here to download high resolution image

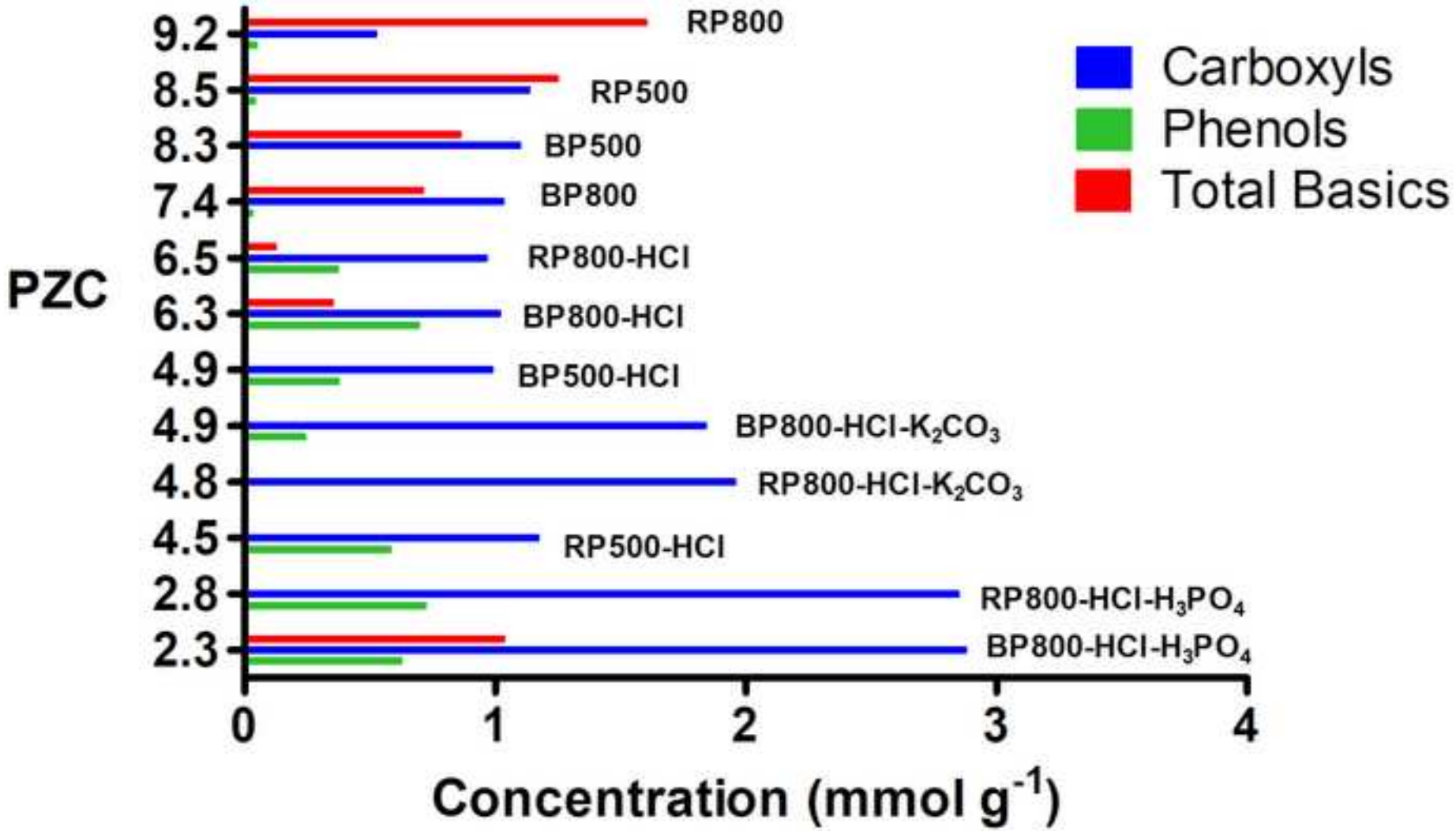

Figure 2

Click here to download high resolution image

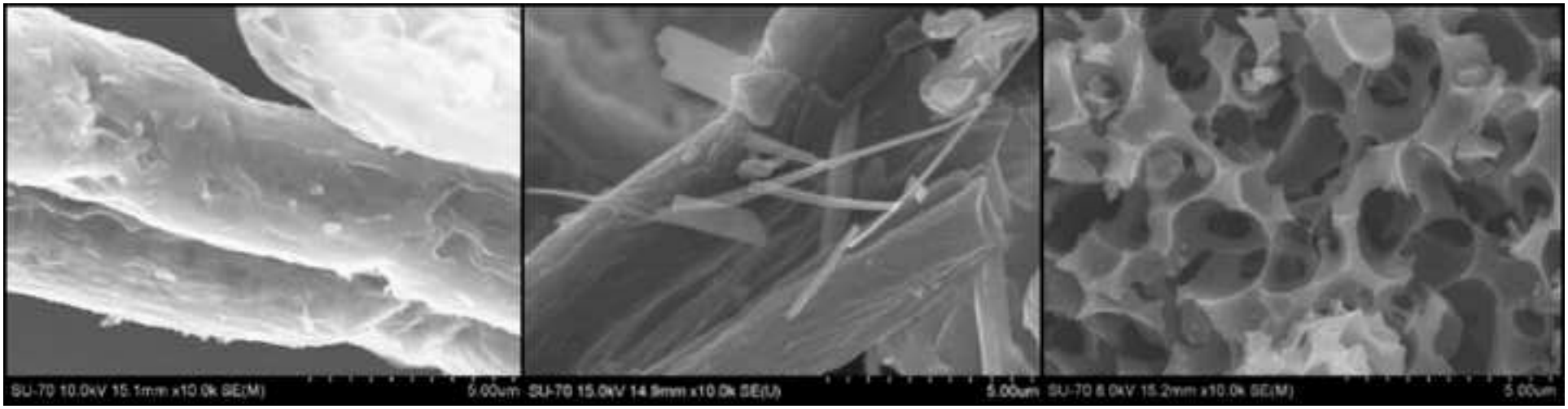

Figure 3

Click here to download high resolution image

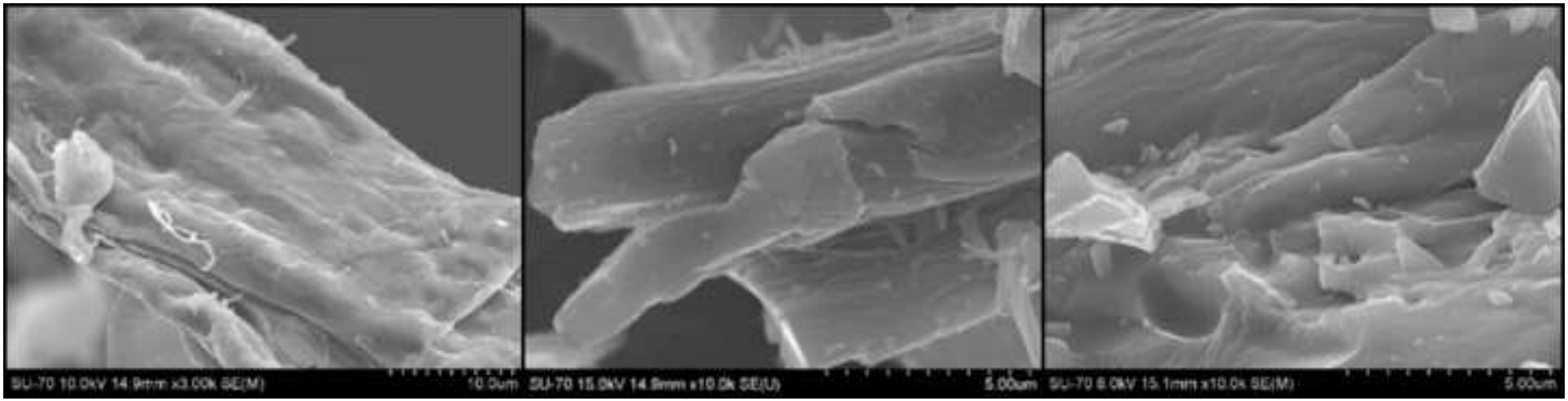

Figure 4 b&w

Click here to download high resolution image

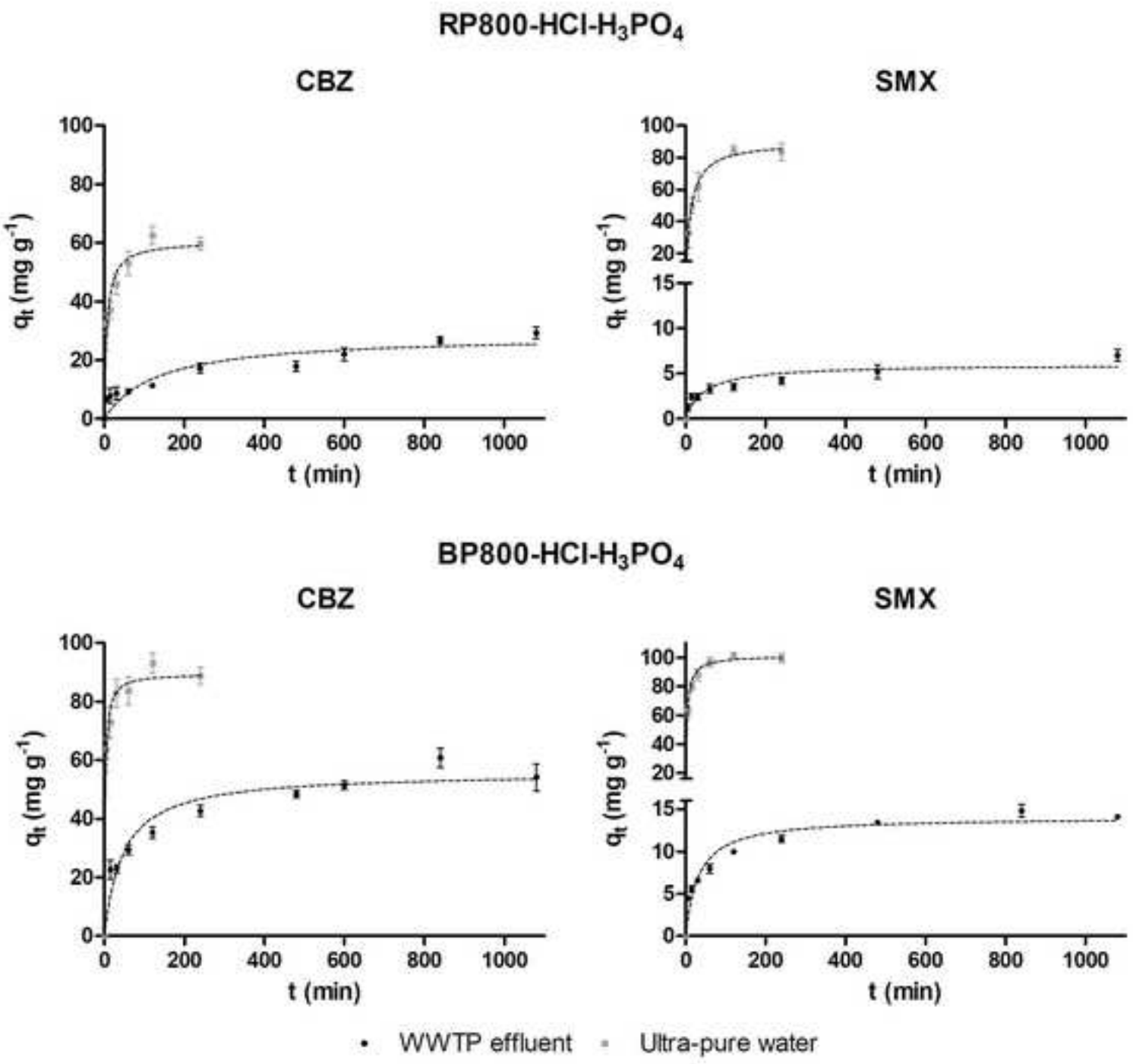

Figure 4 color

Click here to download high resolution image

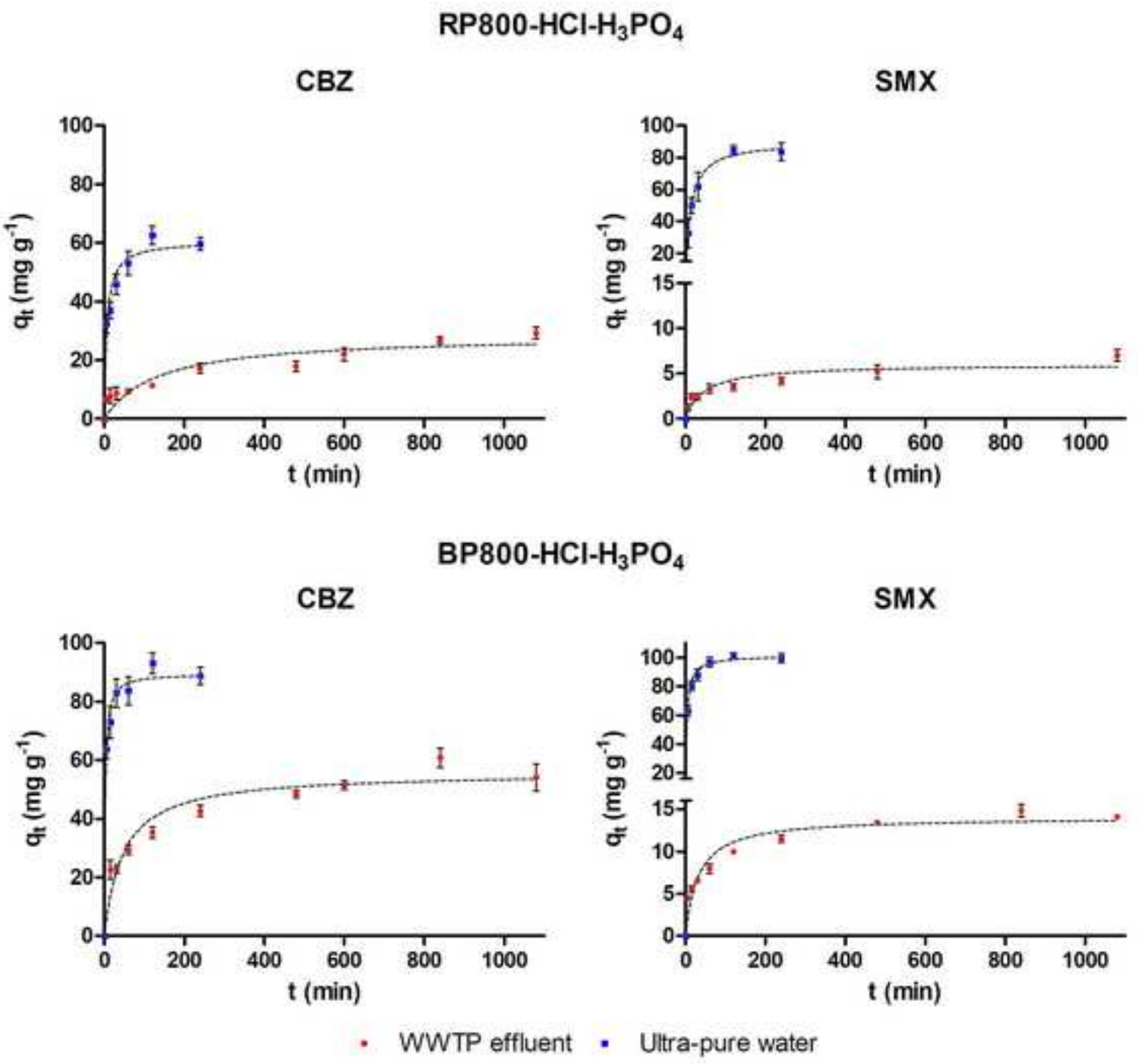

Figure 5 b&w

Click here to download high resolution image

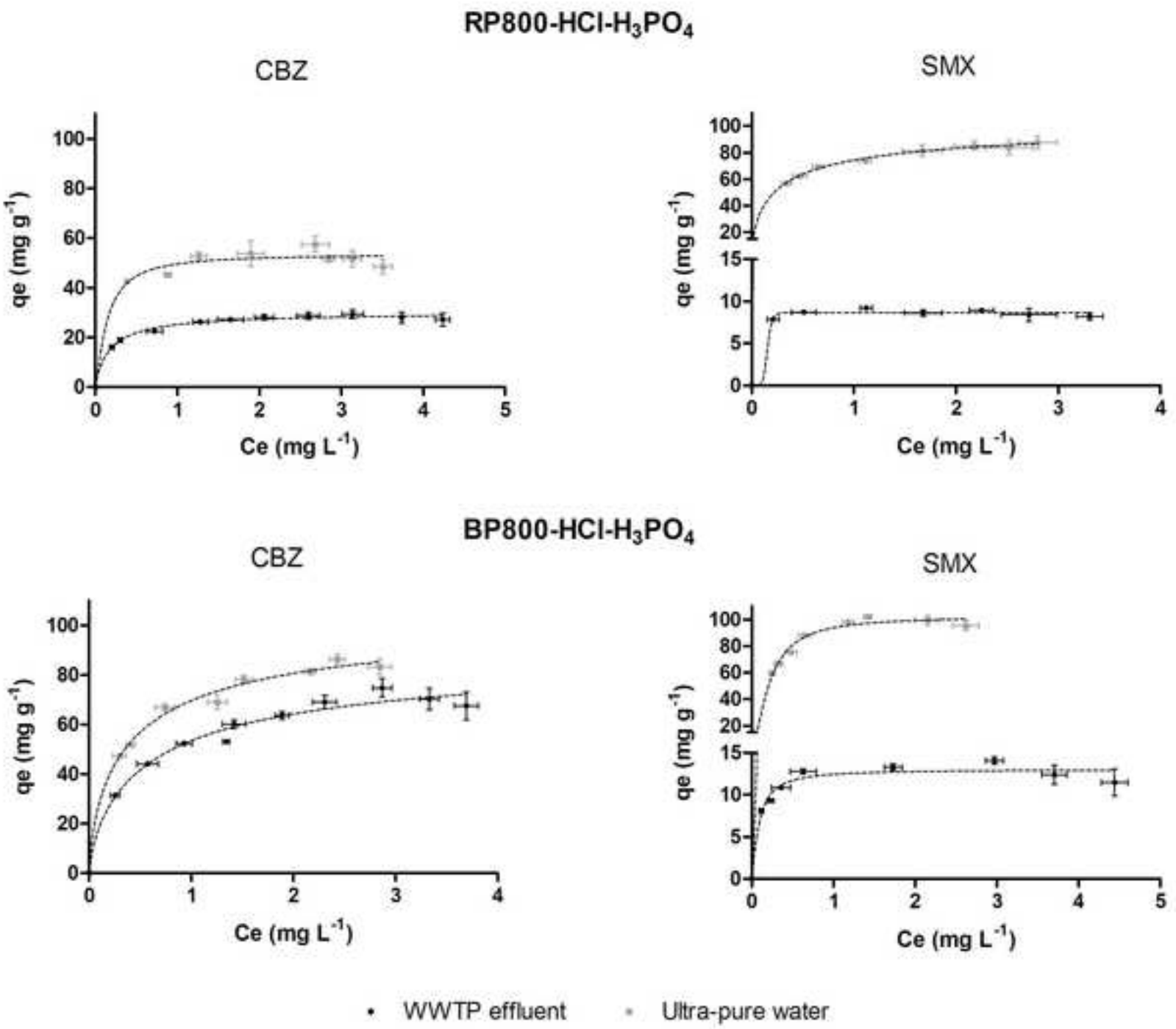

Figure 5 color

Click here to download high resolution image

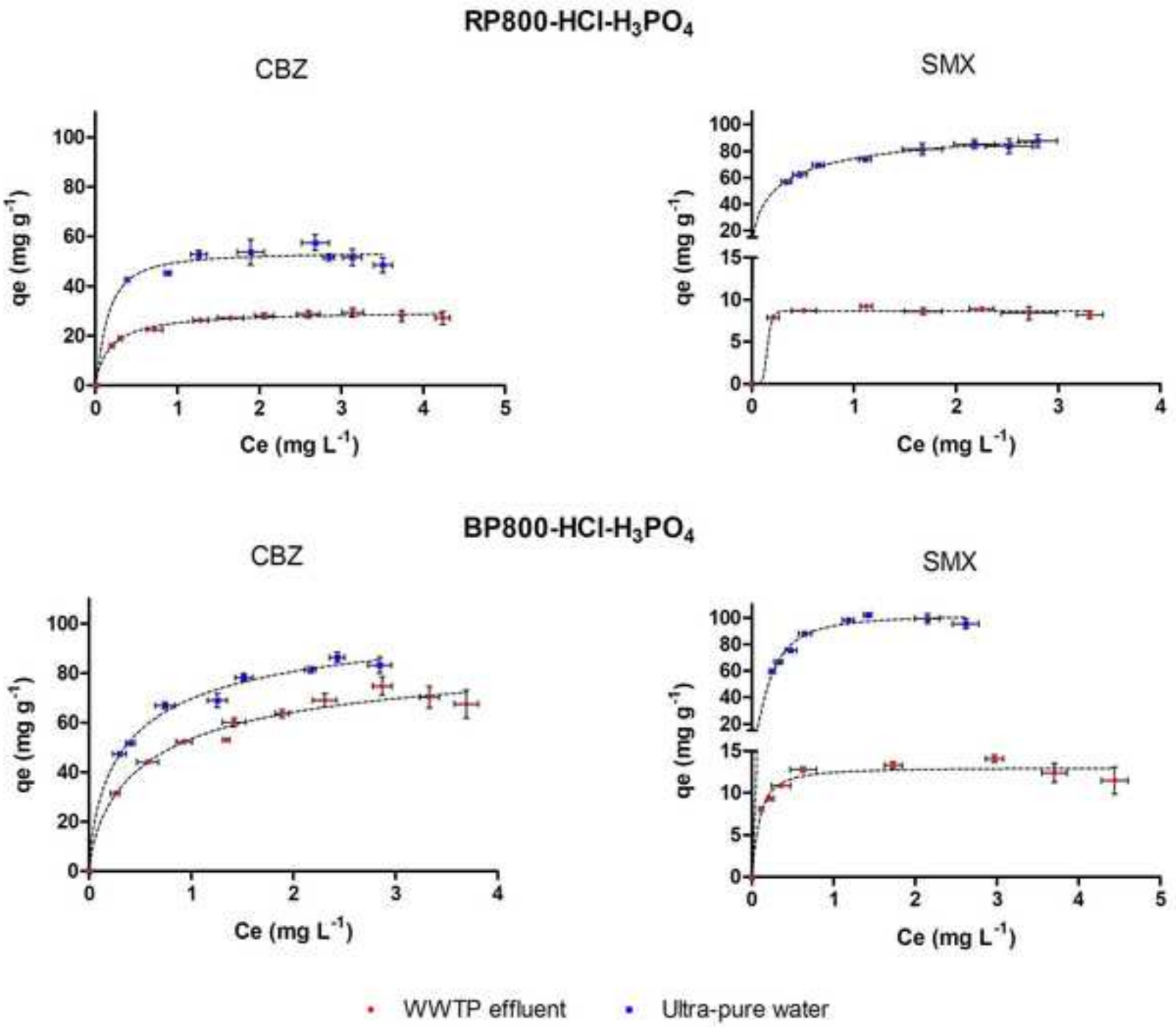

Figure 6

Click here to download high resolution image

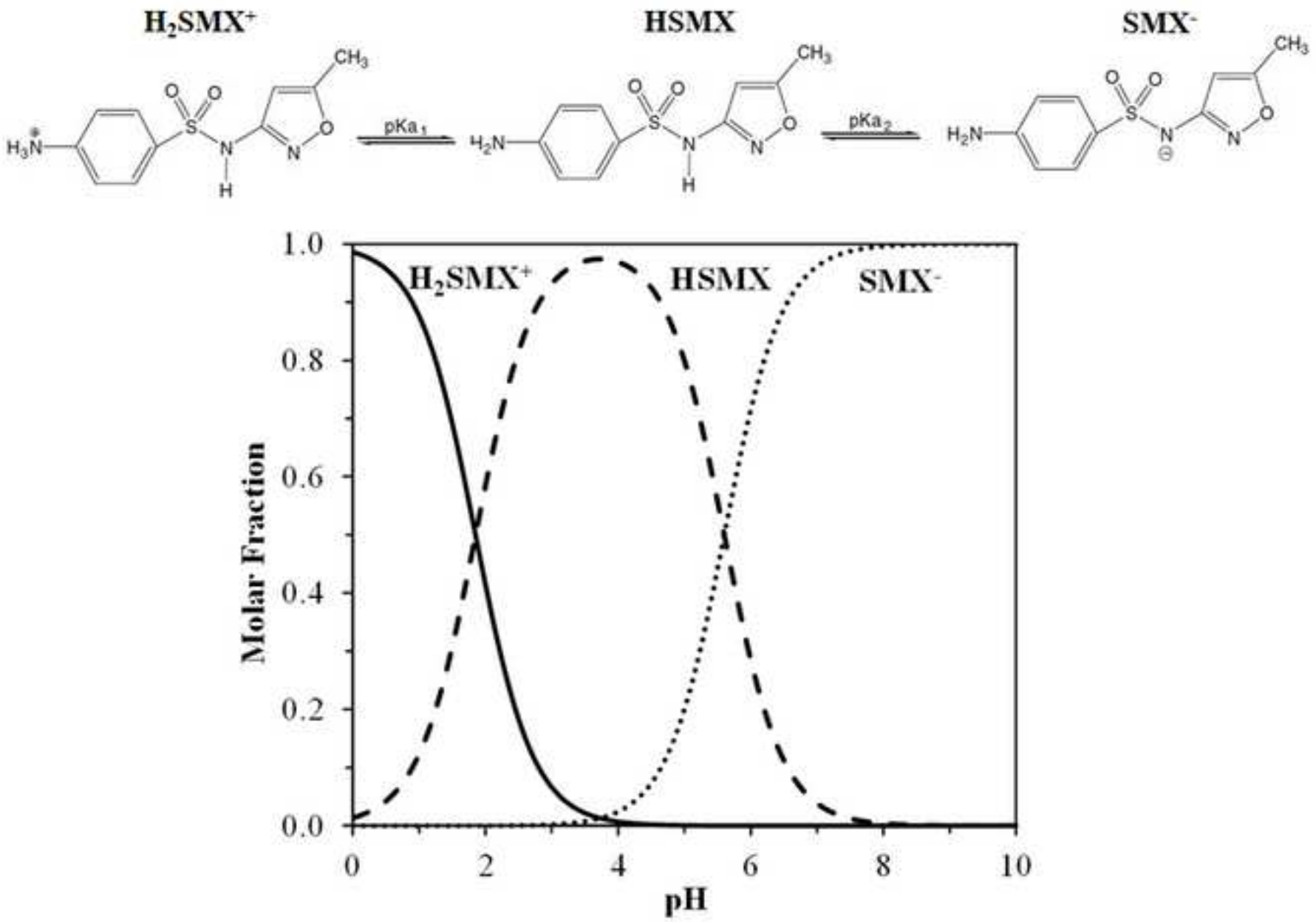

Supplementary material for on-line publication only

Click here to download Supplementary material for on-line publication only: Supporting_Information.docx